

Synthesis of B- and P-Heterocycles by Reaction of Cyclic Acetals and Ketals with Borinium and Phosponium Ions

Feng Wang,[†] W. Andy Tao,[†] Fábio C. Gozzo,[‡] Marcos N. Eberlin,[‡] and R. Graham Cooks*[†]

Department of Chemistry, Purdue University, West Lafayette, Indiana 47907-1393, and State University of Campinas-UNICAMP, Institute of Chemistry, CP 6154, SP 13083-970, Brazil

Received December 15, 1998

Tricoordinated cyclic boron cations result from gas-phase ion/molecule reactions of dicoordinated borinium ions with neutral acetals and ketals and thiazolidine. The reaction, which proceeds via initial cationic binding to a heteroatom followed by a consecutive ring-opening and ring-reclosing process, resembles the Eberlin transacetalization of acylium ions (Eberlin, M. N.; Cooks, R. G. *Org. Mass Spectrom.* **1993**, *28*, 679). The cyclic structure of the tricoordinated boron cation is demonstrated by tandem mass spectrometry and further confirmed by comparison with authentic cyclic tricoordinated boron cations. The five-membered cyclic boron cations dissociate by ethylene oxide loss to thus reform the reactant-dicoordinated borinium ion; the six-membered boron cations fragment instead by ethylene loss. Consistent with the proposed mechanism, the ion/molecule reaction efficiency falls in the order $\text{CH}_3\text{OB}^+\text{C}_2\text{H}_5 > \text{CH}_3\text{OB}^+\text{OCH}_3 \gg \text{CH}_3\text{B}^+\text{CH}_3$; i.e., the higher the nucleophilicity of the borinium ion, the higher the reaction efficiency. A potential energy surface is calculated for the reaction of $\text{CH}_3\text{OB}^+\text{OCH}_3$ with 2-methyl-1,3-dioxolane, and the reaction is found to be 43.3 kcal/mol exothermic due to initial formation of a strong B–O bond. The analogous reactivity displayed by phosphonium ions is also investigated by both experiment and ab initio calculations. In contrast to the borinium ions, the phosphonium ions exhibit higher regioselectivity for sulfur compared to nitrogen and oxygen. Finally, the present findings indicate that the reaction exothermicity and the regioselectivity are controlled by both the Lewis acidity of the reactant cations and the leaving ability of the released neutrals in the rate-limiting nucleophilic-induced recyclization step.

Introduction

Dicoordinated borinium ions ($\text{R}-\text{B}^+-\text{R}$) are of interest as intermediates in nucleophilic reactions of neutral boranes.^{1–5} With two empty p-orbitals on the boron, these strong Lewis acids are extremely reactive with solvent molecules and counterions, a situation that leads to condensed-phase studies of borinium ions being limited to those bearing substituents capable of π -back-bonding or steric shielding.⁴ In contrast to the condensed-phase work, simple borinium ions are readily generated in the gas phase by electron ionization of boron-containing organic molecules,^{6–9} and gas-phase ion chemistry studies have provided invaluable insights into the intrinsic chemical reactivities of borinium ions, including those with no π -back-bonding or steric shielding substituents.^{10–14}

Gas-phase reactions of the dimethoxyborinium ion ($\text{CH}_3\text{OB}^+\text{OCH}_3$) with ethers,¹⁵ alcohols,¹⁶ diols,^{17,18} amides,¹⁹ quionones,²⁰ long-chain carboxylic esters,²¹ and barbiturates²² have been thoroughly investigated. In reactions with alcohols and ethers, $\text{CH}_3\text{OB}^+\text{OCH}_3$ rapidly abstracts water via elimination of one and two alkene molecules, respectively, through proton-bound intermediates.^{15,16} Kenttämaa and co-workers found that $\text{CH}_3\text{OB}^+\text{OCH}_3$ reacts only with *cis*-diols via adduct formation followed by an intramolecular displacement of methanol, and this stereospecificity serves to differentiate stereoisomeric diols.¹⁸ Furthermore, $\text{CH}_3\text{OB}^+\text{OCH}_3$ adducts of long-chain carboxylic esters produce one primary product ion, the acylium ion, and a single secondary ion, the

* To whom correspondence should be addressed. Tel: (765) 494-5262. Fax: (765) 494-0239. E-mail: cooks@purdue.edu.

[†] Purdue University.

(1) Higashi, J.; Eastman, A. D.; Parry, R. W. *Inorg. Chem.* **1982**, *21*, 716.

(2) Nöth, H.; Staudigl, R.; Wagner, H.-U. *Inorg. Chem.* **1982**, *21*, 706.

(3) Nöth, H.; Weber, S.; Rasthofer, B.; Narula, C.; Konstantinov, A. *Pure Appl. Chem.* **1983**, *55*, 1453.

(4) Kölle, P.; Nöth, H. *Chem. Rev.* **1985**, *85*, 399.

(5) Schneider, W. F.; Narula, C. K.; Noth, H.; Bursten, B. *Inorg. Chem.* **1991**, *30*, 3919.

(6) Law, R.; Margrave, J. L. *J. Chem. Phys.* **1956**, *25*, 1086.

(7) Wada, Y.; Kiser, R. W. *J. Phys. Chem.* **1964**, *68*, 1588.

(8) Fallon, P. J.; Kelly, P.; Lockhart, J. C. *Int. J. Mass Spectrom. Ion Phys.* **1968**, *1*, 133.

(9) Cragg, R. H.; Todd, J. F. J.; Weston, A. F. *J. Chem. Soc., Dalton Trans.* **1972**, 1373.

(10) Murphy, M. K.; Beauchamp, J. L. *J. Am. Chem. Soc.* **1976**, *98*, 1433.

(11) Kappes, M. M.; Uppal, J. S.; Staley, R. H. *Organometallics* **1982**, *1*, 1303.

(12) Forte, L.; Lien, M. H.; Hopkinson, A. C.; Bohme, D. K. *Can. J. Chem.* **1990**, *68*, 1629.

(13) Ranatunga, T. D.; Poutsma, J. C.; Squires, R. R.; Kenttämaa, H. I. *Int. J. Mass Spectrom. Ion Processes* **1993**, *128*, L1.

(14) Hettich, R. L.; Cole, T.; Freiser, B. S. *Int. J. Mass Spectrom. Ion Processes* **1987**, *81*, 203.

(15) Ranatunga, T. D.; Kenttämaa, H. I. *J. Am. Chem. Soc.* **1992**, *114*, 8600.

(16) Ranatunga, T. D.; Kenttämaa, H. I. *Inorg. Chem.* **1995**, *34*, 18.

(17) Hua, S.; Chen, Y.; Jiang, L.; Xue, S. *Org. Mass Spectrom.* **1985**, *20*, 719.

(18) Leeck, D. T.; Ranatunga, T. D.; Smith, R. L.; Partanen, T.; Vainiotalo, P.; Kenttämaa, H. I. *Int. J. Mass Spectrom. Ion Processes* **1995**, *141*, 229.

(19) Nanayakkara, V. K.; Kenttämaa, H. I. *Proc. 42nd ASMS Conf. Mass Spectrom. Allied Top.* **1994**, 737.

(20) Hall, B. J.; Brodbelt, J. S. *Int. J. Mass Spectrom. Ion Processes* **1996**, *155*, 123.

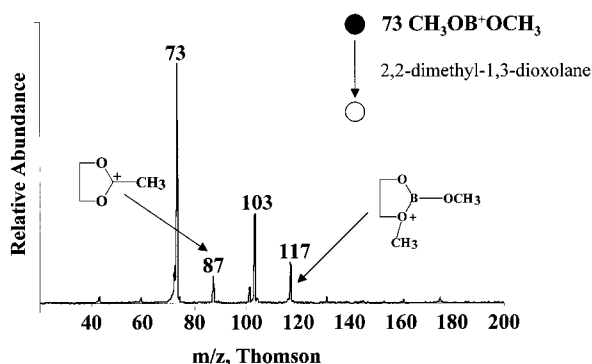
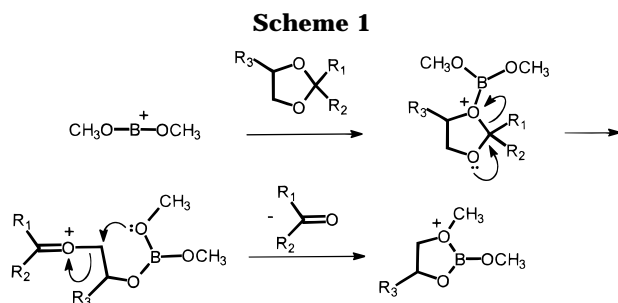
(21) Thoen, K. K.; Tutko, D.; Ranatunga, T. D.; Kenttämaa, H. I. *J. Am. Soc. Mass Spectrom.* **1996**, *7*, 1138.

(22) Colorado, A.; Brodbelt, J. *J. Mass Spectrom.* **1996**, *31*, 403.

Table 1. Products of Ion/Molecule Reactions with the Borinium Ion $\text{CH}_3\text{OB}^+\text{OCH}_3$ (m/z 73)

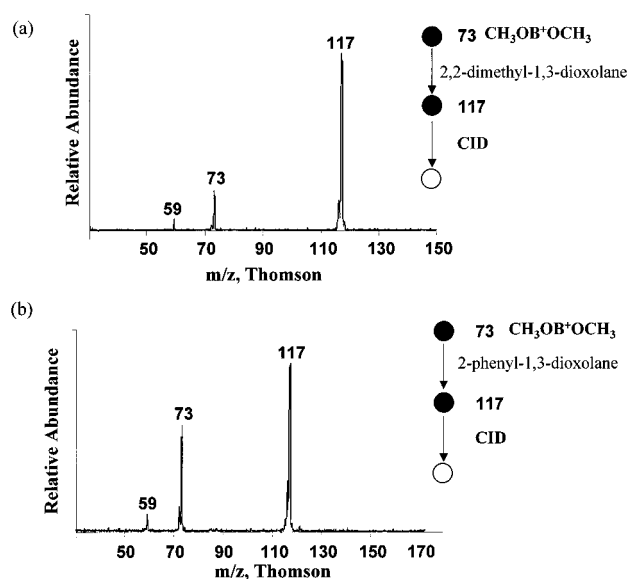
compd	MW	products m/z (rel abundance)			
		transacetalization ^a	proton transfer	H (or alkyl) abstraction	other products
1,3-dioxolane	74	117 (100)	75 (72)	N/A	89 (39), 103 (11), 119 (44)
2-methyl-1,3-dioxolane	88	117 (100)	89 (69)	87 (41)	103 (48), 129 (4), 131 (9), 147 (4)
2,2-dimethyl-1,3-dioxolane	102	117 (50)	103 (100)	101 (20), 87 (33)	131 (7)
2-phenyl-1,3-dioxolane	150	117 (100)	151 (90)	149 (33)	121 (95)
4-methyl-1,3-dioxolane	88	131 (10)	89 (17)	87 (100)	101 (2), 103 (2), 105 (3), 133 (19)
1,3-dioxane	88	131 (20)	89 (20)	87 (100)	103 (19), 133 (14), 145 (29), 173 (8)
thiazolidine	89	116 (37), ^b 133 (47) ^c	90 (74)	88 (21)	102 (58), 118 (100), 130 (95), 162 (53)

^a C–O by B–O replacement formally analogous to transacetalization. ^b C–S by B–O replacement formally analogous to transacetalization. ^c C–N by B–O replacement formally analogous to transacetalization.

**Figure 1.** Product ion (MS^2) spectrum showing ion/molecule reactions of $\text{CH}_3\text{OB}^+\text{OCH}_3$ with 2,2-dimethyl-1,3-dioxolane.

protonated ester.²¹ Meanwhile, adducts of $\text{CH}_3\text{OB}^+\text{OCH}_3$ with barbiturates were found to dissociate by elimination of methanol followed by attachment of a trimethylborate or water molecule in a secondary ion/molecule reaction.²²

Recently, reactions of $\text{CH}_3\text{OB}^+\text{OCH}_3$ were proposed for the MS structural characterization of unknown carbonyl compounds.²³ This ion readily attacks carbonyl compounds and cleaves C=O and C–C bonds to form competing hydroxy and aldehyde abstraction products via 1,2-hydride shifts in the primary adduct. Kempen and Brodbelt extended the use of $\text{CH}_3\text{OB}^+\text{OCH}_3$ to the analysis of biologically active molecules.²⁴ More recently, dissociation of $\text{CH}_3\text{OB}^+\text{OCH}_3$ -bound pyridine dimers provided the relative borinium ion affinities of variously substituted pyridines.²⁵ Agostic bonding (C–H...O) between an ortho substituent and the oxygen of the central binding borinium ion has been recognized from the gas-phase stereoelectronic parameters measured from the relative rates of dissociation of the cation-bound dimer.²⁶

**Figure 2.** Sequential product ion (MS^3) spectra of the proposed transacetalization products of $\text{CH}_3\text{OB}^+\text{OCH}_3$ with (a) 2,2-dimethyl-1,3-dioxolane and (b) 2-phenyl-1,3-dioxolane.

An equilibrium study on the binding of $\text{CH}_3\text{OB}^+\text{OCH}_3$ to the substituted pyridines also established that association is sensitive to the substituents near the site of ion attachment.²⁷ These studies demonstrate that the binding energy of $\text{CH}_3\text{OB}^+\text{OCH}_3$ to neutral ligands is controlled by both steric and electronic effects.

Gas-phase acylium ($\text{RC}^+=\text{O}$)^{28,29} and related sulfinyl cations ($\text{RS}^+=\text{O}$)³⁰ undergo the gas-phase Eberlin transacetalization reaction³¹ with acetals and ketals. In analogy to the protection of neutral ketones in the condensed phase, the resulting cyclic 1,3-dioxolanylium ions serve as “ionic ketals” to protect acylium ions in the gas phase. Also interesting is the fact that collision-induced dissociation of the cyclic “ionic ketals” reforms the acylium ions in high yield, a step that is comparable to the hydrolysis of neutral acetals and ketals in the condensed phase. To further expand, and generalize, the Eberlin reaction,³¹ the reactions of $\text{CH}_3\text{OB}^+\text{OCH}_3$ with various acetals and ketals, and thiazolidine, are now subjected to a detailed investigation by multiple-stage mass spec-

(27) Isbell, J. J.; Brodbelt, J. S. *Rapid Commun. Mass Spectrom.* **1996**, *10*, 1418.

(28) Eberlin, M. N.; Cooks, R. G. *Org. Mass Spectrom.* **1993**, *28*, 679.

(29) Moraes, L. A. B.; Gozzo, F. C.; Eberlin, M. N.; Vainiotalo, P. J. *Org. Chem.* **1997**, *62*, 5096.

(30) Gozzo, F. C.; Sorriha, P. M.; Eberlin, M. N. *J. Chem. Soc., Perkin Trans. 2* **1996**, 587.

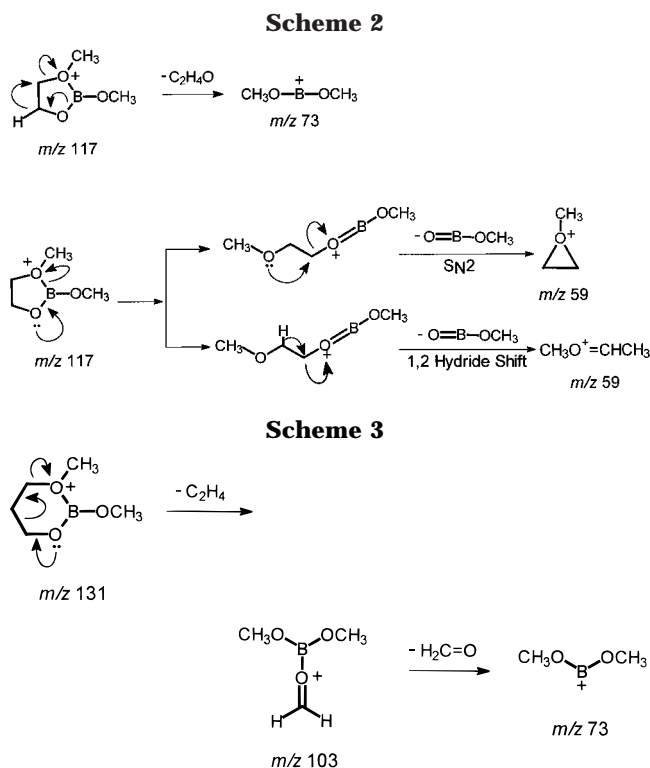
(31) Wang, F.; Ma, S.; Tao, W. A.; Cooks, R. G. *Angew. Chem., Int. Ed. Engl.* **1999**, *38*, 386.

(23) Ranatunga, T. D.; Kennady, J. M.; Kenttamaa, H. I. *J. Am. Chem. Soc.* **1997**, *119*, 5200.

(24) Kempen, E.; Brodbelt, J. J. *Mass Spectrom.* **1997**, *32*, 846.

(25) Ma, S.; Wong, P.; Cooks, R. G. *J. Mass Spectrom.* **1997**, *32*, 159.

(26) Eberlin, M. N.; Kotiah, T.; Shay, B. J.; Yang, S. S.; Cooks, R. G. *J. Am. Chem. Soc.* **1994**, *116*, 2457.



trometry (MS^2 and MS^3). A highly exothermic reaction channel leading to the generation of cyclic tricoordinated boron cations is discovered, and product ion structures are characterized by low energy collision-induced dissociation (CID). A reaction mechanism is proposed in which cyclic tricoordinated boron cations are formed via electrophilic attachment of $CH_3OB^+OCH_3$ to the heteroatom, followed by consecutive ring opening and intramolecular nucleophilic-induced ring recyclization with the elimination of a carbonyl compound, or its neutral analogue. This mechanism is corroborated by the finding of an interesting dependence of reaction efficiency on nucleophilicity of the reactant borinium ions and independently, by ab initio molecular orbital calculations.

A preliminary report has appeared on the reactions of related phosphonium ions, i.e., $CH_3P^+(O)OCH_3$ and $CH_3-OP^+(O)OCH_3$, which initiate efficient C–O by P–O replacement in five-membered cyclic acetals and ketals.³¹ (A somewhat related reaction has been utilized in the multiple-step synthesis of 1-*O*-acylglycerol-2,3-cyclic phosphate in solution.³²) The resulting 1,3,2-dioxaphospholanium ion fragments mainly to regenerate the reactant phosphonium ion. Correspondingly, 1,3,2-dioxaphospholanes are often hydrolyzed or photolyzed back to the initial phosphonium ions in the condensed phase.³³ Owing to the polarity of the P–O bond, the 1,3,2-dioxaphospholanium ion undergoes double-hydrogen transfer to give an additional fragment ion, the abundance of which is very sensitive to the substituents on the reactant phosphonium ions.³¹ To further elucidate the details of the C–O by P–O replacement and the regioselectivity associated with the phosphoryl group, we have calculated intrinsic reaction coordinates (IRC) for the reactions of

(32) Kobayashi, S.; Tokunoh, R.; Shibasaki, M.; Shinagawa, R.; Murakami-Murofushi, K. *Tetrahedron Lett.* **1993**, *34*, 4047.

(33) Corbridge, D. E. C. *Phosphorus: An Outline of Its Chemistry, Biochemistry and Uses*, 5th ed.; Elsevier Science B.V.: Amsterdam, 1995.

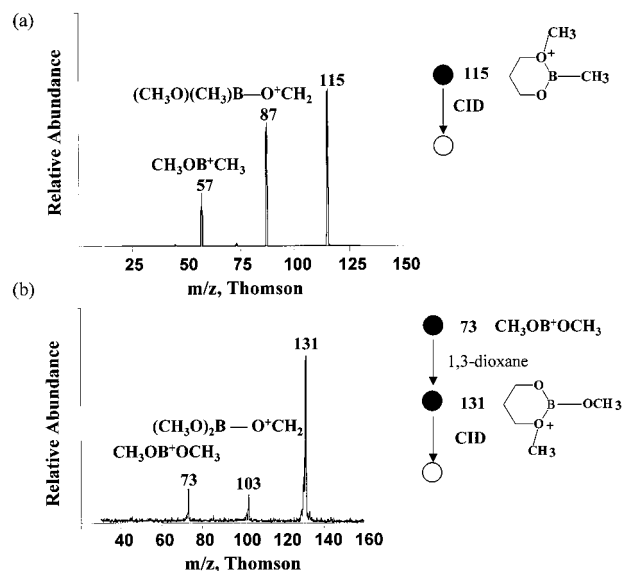


Figure 3. (a) Collision-induced dissociation spectrum (CID) of methylated 1,3-dioxaborinane. (b) Sequential product ion (MS^3) spectrum of the tricoordinated boron cation generated by reaction of $CH_3OB^+OCH_3$ with 1,3-dioxane.

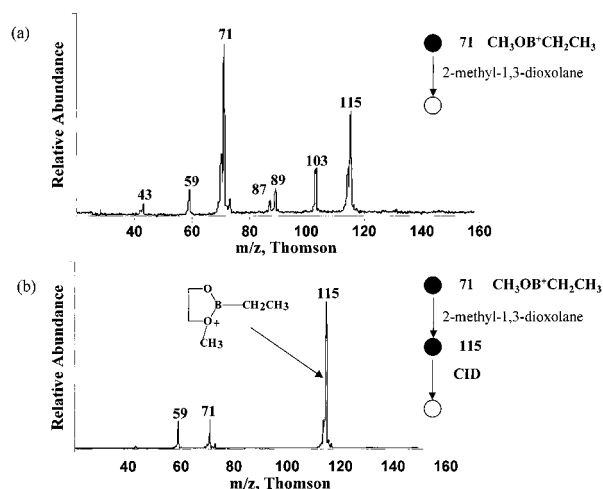


Figure 4. (a) Product ion (MS^2) spectrum showing ion/molecule reactions of $CH_3OB^+CH_2CH_3$ with 2-methyl-1,3-dioxolane. (b) Sequential product ion (MS^3) spectrum of the transacetalization product of m/z 115.

the phosphonium ions with 2-methyl-1,3-dioxolane and 1,3-oxathiolane. Most importantly, this report demonstrates that B–O and P–O bonds can be directly incorporated to the cyclic acetals and ketals by using the appropriate reagent ions. The driving force is the formation of an initial ion/molecule adduct with a strong dative B–O or P–O bonding.

Experimental and Theoretical Methods

All experiments were performed using a home-built pentapole mass spectrometer comprised of three mass-analyzing quadrupoles (Q1, Q3, Q5) and two reaction quadrupoles (Q2, Q4).³⁴ For MS^2 experiments, the reactant ion was mass-selected by using Q1 and then allowed to undergo ion/molecule reactions with the neutral reagent introduced into Q2. The ion/molecule reaction products were recorded by

(34) Schwartz, J. C.; Schey, K. L.; Cooks, R. G. *Int. J. Mass Spectrom. Ion Processes* **1990**, *101*, 1.

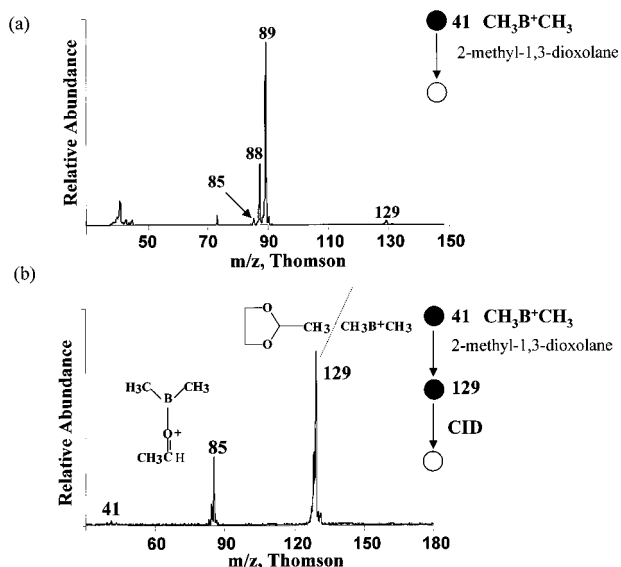


Figure 5. (a) Product ion (MS²) spectrum showing ion/molecule reactions of CH₃B⁺CH₃ with 2-methyl-1,3-dioxolane. (b) Sequential product ion (MS³) spectrum of the intact adduct, *m/z* 129.

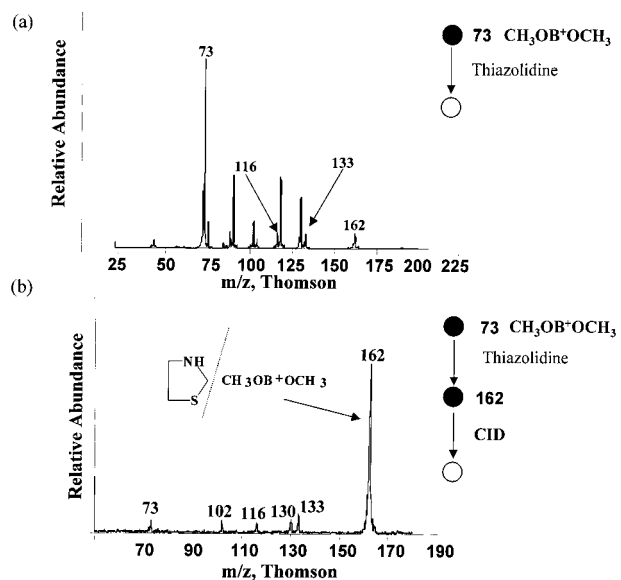


Figure 6. (a) Product ion (MS²) spectrum showing ion/molecule reactions of CH₃OB⁺OCH₃ with thiazolidine. (b) Sequential product ion (MS³) spectrum of the intact adduct, *m/z* 162.

scanning Q5 with both Q3 and Q4 set in the broad-band rf-only mode. The boron- or phosphorus-containing products formed in Q2 were characterized in MS³ experiments, in which they were mass-selected by using Q3 and then allowed to undergo energetic collisions with argon in Q4, while Q5 was scanned to record the sequential product ion MS³ spectrum. Typical reaction energy in Q2 and collision energy in Q4 are 0 and 10 eV (under multiple collision conditions, more than 40% beam attenuation), respectively.

The reactant cations CH₃OB⁺OCH₃, CH₃P⁺(O)OCH₃, and CH₃OP⁺(O)OCH₃ were generated by standard 70 eV electron ionization of trimethylborate and dimethyl methyl phosphonate, respectively. All compounds were commercially available and used without further purification. The mass/charge ratio (*m/z*) is reported using the Thomson unit (1 Th = 1 atomic mass per unit positive charge³⁵).

Ab initio molecular orbital calculations were carried out using standard procedures in the Gaussian 94 suite of pro-

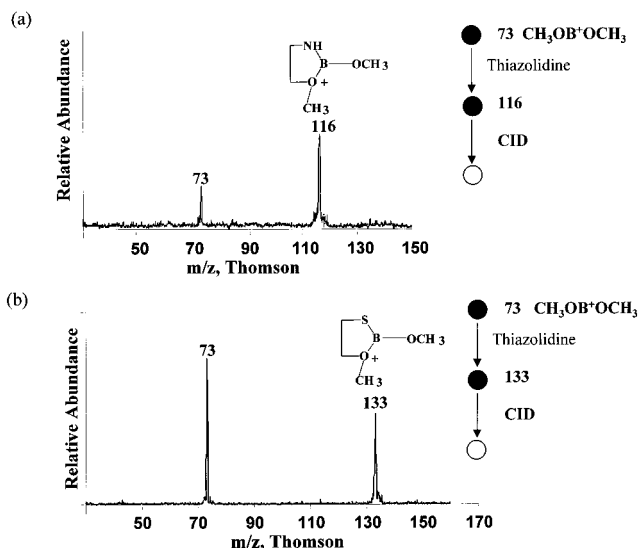
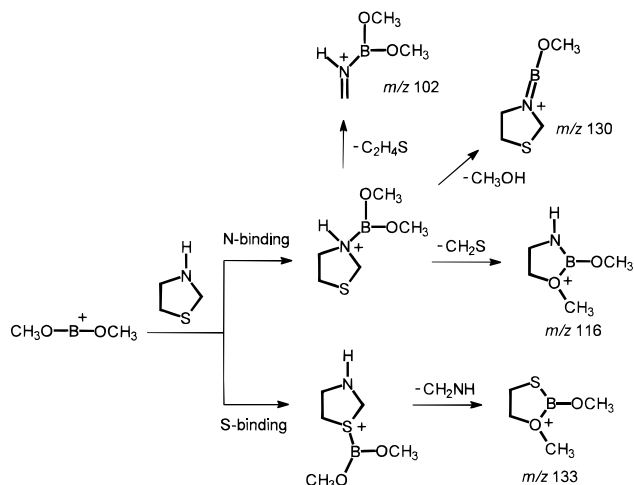


Figure 7. Sequential product ion (MS³) spectrum of the transacetalization products of CH₃OB⁺OCH₃ attacking thiazolidine at the (a) N site and (b) S site.

Scheme 4



grams.³⁶ The closed-shell ions were optimized at the restricted (RHF) Hartree-Fock level of theory by employing the polarization 6-31G(d,p) basis set.³⁷ Single-point energies were obtained by second-order Møller-Plesset (MP2) perturbation theory³⁸ using the RHF/6-31G(d,p)-optimized geometries, a procedure denoted as MP2(FC)/6-31G(d,p)//RHF/6-31G(d,p). Harmonic vibrational frequencies were calculated at the RHF/6-31G(d,p) level to characterize the stationary points and to obtain the zero-point vibrational energies, which were scaled by a factor of 0.89 in the final total energy calculations. Complete structural parameters, total energies, and lists of vibrational frequencies for all RHF/6-31G(d,p)-optimized structures are available upon request.

(35) Cooks, R. G.; Rockwood, A. L. *Rapid Commun. Mass Spectrom.* **1991**, *5*, 93.

(36) Gaussian 94, Revision D.2: Frisch, M. J.; Trucks, G. W.; Schlegel, H. B.; Gill, P. M. W.; Johnson, B. G.; Robb, M. A.; Cheeseman, J. R.; Keith, T.; Petersson, G. A.; Montgomery, J. A.; Raghavachari, K.; Al-Laham, M. A.; Zakrzewski, V. G.; Ortiz, J. V.; Foresman, J. B.; Cioslowski, J.; Stefanov, B. B.; Nanayakkara, A.; Challacombe, M.; Peng, C. Y.; Ayala, P. Y.; Chen, W.; Wong, M. W.; Andres, J. L.; Replogle, E. S.; Gomperts, R.; Martin, R. L.; Fox, D. J.; Binkley, J. S.; Defrees, D. J.; Baker, J.; Stewart, J. P.; Head-Gordon, M.; Gonzalez, C.; Pople, J. A. Gaussian, Inc., Pittsburgh, PA, 1995.

(37) Hehre, W. J.; Ditchfield, R.; Pople, J. A. *J. Chem. Phys.* **1972**, *56*, 2257.

(38) Møller, C.; Plesset, M. S. *Phys. Rev.* **1934**, *46*, 618.

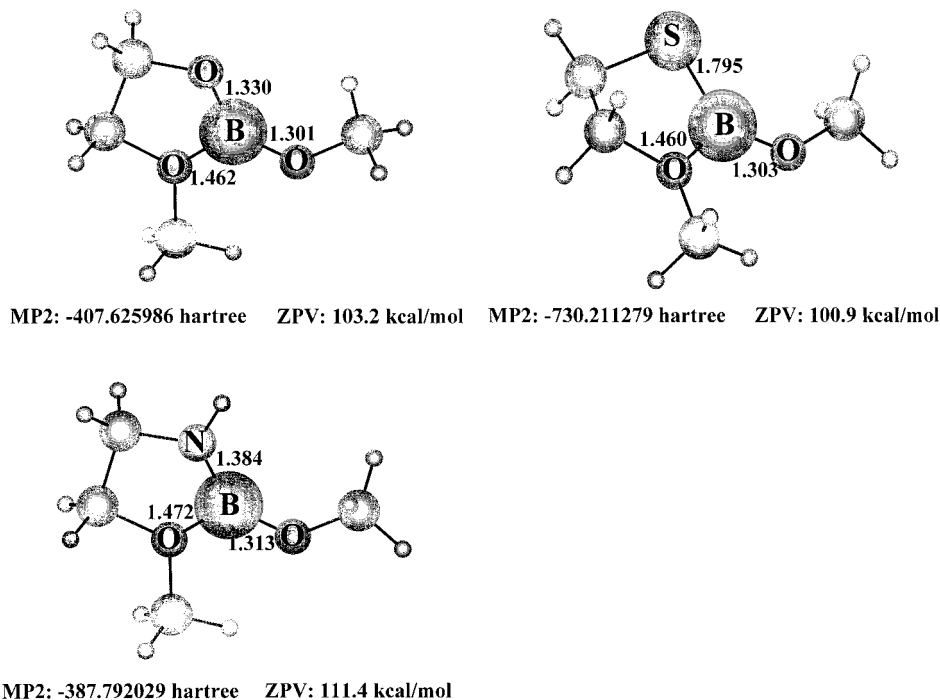


Figure 8. RHF/6-31G(d,p)-optimized structures of tricoordinated boron cations.

Results and Discussion

1. Reactions with Borinium Ions. 1.1. C–O by B–O Replacement. The reactions of the mass-selected dimethoxyborinium ion $\text{CH}_3\text{OB}^+\text{OCH}_3$ (m/z 73) with a series of neutral cyclic acetals and ketals display products generated via proton (or alkyl) transfer, deprotonation, and other reactions. Reaction products are listed in Table 1, and a typical MS^2 product ion spectrum, represented by the reaction of $\text{CH}_3\text{OB}^+\text{OCH}_3$ with 2,2-dimethyl-1,3-dioxolane, is shown in Figure 1. An ionic product of major interest is that of m/z 117, which is likely produced via elimination of acetone (58 mass units) from the activated intact adduct of m/z 175. This type of process, i.e., addition followed by elimination of a neutral aldehyde or ketone, occurs generally for other acetals and ketals, and the corresponding product ions are formed with high yield (Table 1). Scheme 1 presents a general mechanism proposed for the apparent transformation of neutral acetals and ketals to the tricoordinated cyclic boron cations. This mechanism, which involves two key steps, electrophilic ring opening and nucleophilic-induced recyclization, resembles that proposed for transacetalization of acylium ions.^{28,29,39} A similar reactivity is also observed for thioacylium ions,²⁹ pyridyl cations,⁴⁰ and sulfinyl cations.^{30,41}

With regard to the transacetalization-like reaction of $\text{CH}_3\text{OB}^+\text{OCH}_3$ (Table 1), the following are noted: (i) protonation and deprotonation are the major competing reactions; (ii) deprotonation probably has the relatively larger influence in decreasing the transacetalization reaction yield; (iii) reactions with ketals are more efficient than those with acetals; and (iv) consistent with the

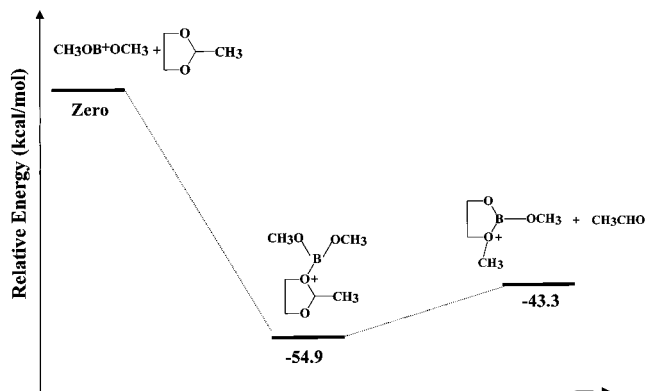


Figure 9. Intrinsic reaction coordinates (IRC) for the transacetalization reaction of $\text{CH}_3\text{OB}^+\text{OCH}_3$ with 2-methyl-1,3-dioxolane.

proposed mechanism (Scheme 1), transacetalization is hampered by substituents at the 4-position of 1,3-dioxolanes due to steric hindrance.

To provide experimental evidence for the proposed mechanism, the product tricoordinated boron cations were mass-selected and interrogated by collision-induced dissociation (MS^3). As Figure 2 exemplifies, in most cases the tricoordinated boron cations fragment mainly to reform the reactant $\text{CH}_3\text{OB}^+\text{OCH}_3$. Reactions of $\text{CH}_3\text{OB}^+\text{OCH}_3$ with alkyl-substituted 1,3-dioxolanes such as 1,3-dioxolane, 2-methyl-1,3-dioxolane, 2,2-dimethyl-1,3-dioxolane, and 2-phenyl-1,3-dioxolane all give, as expected from the mechanism proposed in Scheme 1, the same tricoordinated boron cation of m/z 117, as demonstrated by their identical CID behavior (Figure 2). Upon collisional activation, the m/z 117 ion dissociates by two processes that suggest its cyclic structure (Scheme 2): $\text{C}_2\text{H}_4\text{O}$ loss which forms $\text{CH}_3\text{OB}^+\text{OCH}_3$ (m/z 73) and $\text{O}=\text{B}-\text{OCH}_3$ loss to form $\text{C}_3\text{H}_7\text{O}^+$ (m/z 59). Note that $\text{C}_3\text{H}_7\text{O}^+$ could be generated from the m/z 117 ion by either intramolecular $\text{S}_{\text{N}}2$ to give a methylated oxirane struc-

(39) Eberlin, M. N. *Mass Spectrom. Rev.* **1997**, *16*, 113.

(40) Carvalho, M.; Gozzo, F. C.; Mendes, M. A.; Sparrapan, R.; Kascheres, C.; Eberlin, M. N. *Chem.-Eur. J.* **1998**, *4*, 1161.

(41) Moraes, L. A. B.; Eberlin, M. N. *J. Chem. Soc., Perkin Trans. 2* **1997**, 2105.

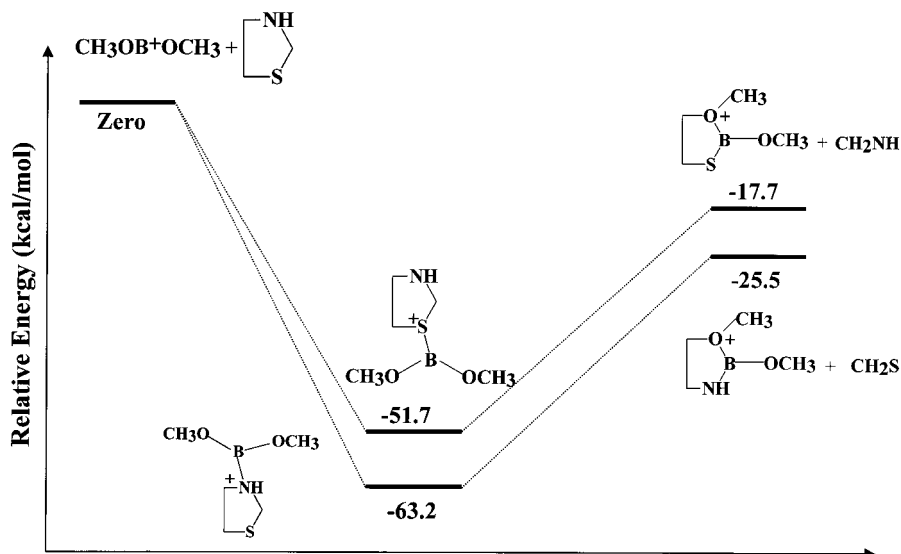


Figure 10. Intrinsic reaction coordinates (IRC) for the transacetalization reaction of $\text{CH}_3\text{OB}^+\text{OCH}_3$ with thiazolidine.

Table 2. Products of Ion/Molecule Reactions with the Phosphonium Ion $\text{CH}_3\text{P}^+(\text{O})\text{OCH}_3$ (m/z 93)

compd	MW	products m/z (rel abundance)			
		transacetalization ^a	proton transfer	H (or alkyl) abstraction	other products
1,3-dioxolane	74	137 (100)	75 (75)	73 (75)	125 (92)
2-methyl-1,3-dioxolane	88	137 (40)	89 (100)	87 (10)	111 (9), 125 (51)
2,2-dimethyl-1,3-dioxolane	102	137 (77)	103 (100)	101 (5), 87 (10)	125 (37), 183 (18)
2-phenyl-1,3-dioxolne	150	137 (100)	N/A	N/A	135 (15)
4-methyl-1,3-dioxolane	88	151 (30)	89 (40)	87 (48)	103 (48), 111 (21), 125 (100), 167 (12), 177 (74), 183 (19)
1,3-oxathiolane	90	153 (100)	N/A	N/A	103 (63), 105 (37), 191 (18)
thiazolidine	89	136 (5), ^b 153 (26) ^c	90 (85)	88 (10)	102 (10), 104 (6), 110 (19), 118 (75)

^a C–O by P–O replacement formally analogous to transacetalization. ^b C–S by P–O replacement formally analogous to transacetalization. ^c C–N by P–O replacement formally analogous to transacetalization.

ture or by 1,2-hydride shift to give the structure $\text{CH}_3\text{-CH}=\text{OCH}_3^+$. According to a recent study of unimolecular dissociation of β -hydroxylated cations by Morton and co-workers,⁴² $\text{C}_3\text{H}_7\text{O}^+$ is most likely to be $\text{CH}_3\text{CH}=\text{OCH}_3^+$. Interestingly, reactions of $\text{CH}_3\text{OB}^+\text{OCH}_3$ with acetaldehyde and methyl ketones occur via two 1,2-hydride shifts in the adducts and give an isomeric product ion of m/z 117, i.e., $(\text{CH}_3\text{O})_2\text{B-O}^+=\text{CHCH}_3$. The structure of the ion was proven by CID; when activated, it yielded two fragments: $\text{CH}_3\text{OB}^+\text{OCH}_3$ (m/z 73) and $\text{CH}_3\text{OB}^+\text{H}$ (m/z 43).²³ Such contrasting dissociation behavior allows ready distinction between the cyclic and acyclic isomers of ion m/z 117.

According to the proposed transacetalization-like mechanism (Scheme 1), a six-membered cyclic tricoordinated boron cation of m/z 131 should result from reaction of $\text{CH}_3\text{OB}^+\text{OCH}_3$ with 1,3-dioxane. This product ion also dissociates by pathways that corroborate the cyclic structure (Scheme 3); that is, via endo-C–O bond cleavage that results in C_2H_4 loss yielding $(\text{CH}_3\text{O})_2\text{B-O}^+=\text{CH}_2$, m/z 103, and further H_2CO loss yielding the reactant ion $\text{CH}_3\text{OB}^+\text{OCH}_3$, m/z 73. To further confirm the cyclic structure, the structurally similar authentic tricoordinated cyclic boron cation, methylated 1,3-dioxaborinane, m/z 115, was generated by chemical ionization of 1,3-dioxaborinane using methyl iodide as reagent gas. Subjected to CID, as expected, the ion of m/z 115 displays dissociation behavior (Figure 3a) similar to that of a

synthetic ion of m/z 131 (Figure 3b) yielding two abundant product ions: $(\text{CH}_3\text{O})(\text{CH}_3)\text{B-O}^+=\text{CH}_2$, m/z 87, and $\text{CH}_3\text{OB}^+\text{CH}_3$, m/z 57. This result provides further experimental evidence for the general chemical transformation mechanism shown in Scheme 1.

The reactivity of dicoordinated borinium ions is dependent on the electron deficiency of the central boron atom. From reactions of five differently substituted boron cations, $\text{CH}_3\text{B}^+\text{CH}_3$, $\text{CH}_3\text{CH}_2\text{B}^+\text{H}$, $\text{CH}_3\text{OB}^+\text{OCH}_3$, $\text{CH}_3\text{-(CH}_2)_2\text{OB}^+\text{OH}$, and $(\text{CH}_3)_2\text{NB}^+\text{N}(\text{CH}_3)_2$, toward a set of oxygen-containing compounds, Kenttämäa and co-workers concluded that $\text{CH}_3\text{B}^+\text{CH}_3$ and $\text{CH}_3\text{CH}_2\text{B}^+\text{H}$ are the most reactive ions due to their greater electron deficiency at the boron center.⁴³ Aiming to investigate the role of oxygen atom in the $\text{CH}_3\text{OB}^+\text{OCH}_3$ ion with respect to the efficiency and the mechanism of the transacetalization-like reaction, reactions with neutral 2-methyl-1,3-dioxolane were performed using $\text{CH}_3\text{OB}^+\text{CH}_2\text{CH}_3$ and $\text{CH}_3\text{B}^+\text{CH}_3$, which were generated from 70 eV electron impact upon $\text{CH}_3\text{OB}(\text{CH}_2\text{CH}_3)_2$ and $(\text{CH}_3)_2\text{BBr}$, respectively. As expected, $\text{CH}_3\text{OB}^+\text{CH}_2\text{CH}_3$ yields the analogous five-membered boron cation of m/z 115 with relatively higher efficiency (Figure 4a). This product dissociates in an MS^3 experiment to give two fragments analogous to those observed for the analogous m/z 117 ion (Figure 2), viz., $\text{CH}_3\text{OB}^+\text{CH}_2\text{CH}_3$ of m/z 71 and $\text{C}_3\text{H}_7\text{O}^+$ of m/z 59, as shown in Figure 4b. $\text{CH}_3\text{B}^+\text{CH}_3$ is, however, much less reactive; its product ion spectrum (Figure 5a) displays two quite minor products: the addition/ $\text{CH}_3\text{C}(\text{O})\text{H}$ elimi-

(42) Nguyen, V.; Bennett, J. S.; Morton, T. H. *J. Am. Chem. Soc.* **1997**, *119*, 8342.

(43) Ranatunga, T. D. Ph.D. Dissertation, Purdue University, 1995.

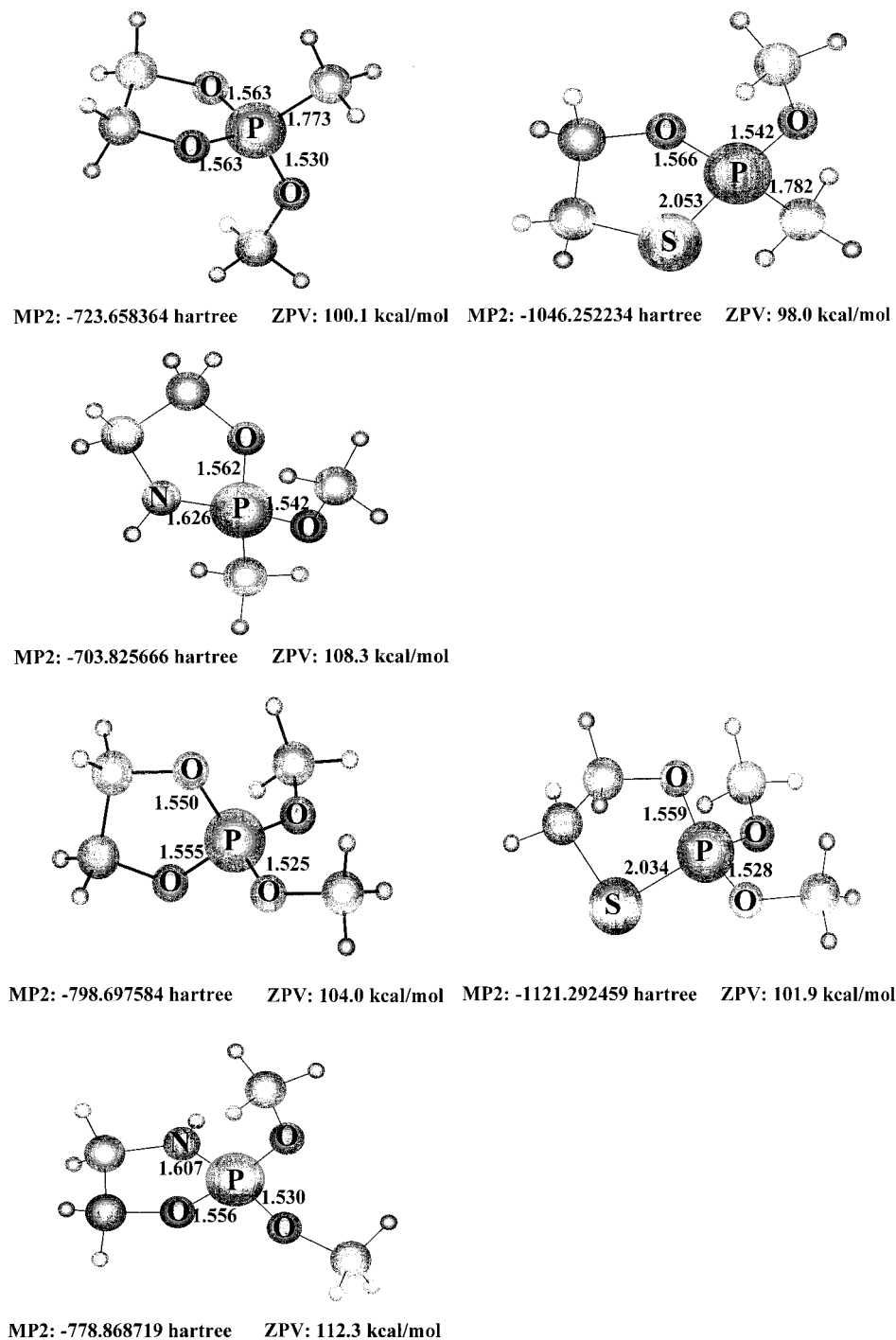


Figure 11. RHF/6-31G(d,p)-optimized structures of 1,3,2-diheterophospholanium ions.

nation product ion of m/z 85 and the intact adduct of m/z 129. Note that intact adducts are barely seen in the ion/molecule reaction spectra of $\text{CH}_3\text{OB}^+\text{OCH}_3$ with cyclic acetals and ketals studied so far. Upon collisional activation, the intact adduct m/z 129 was found to yield two fragments, $(\text{CH}_3)_2\text{B}-\text{OCHCH}_3^+$ of m/z 85 and $\text{CH}_3\text{B}^+\text{CH}_3$ of m/z 41, as shown in Figure 5b. The above observations clearly indicate that the oxygen atom in the reactant boron cation plays an essential role in the transacetalization-like reaction of the borinium ions. Reaction efficiency falls in the order of $\text{CH}_3\text{OB}^+\text{CH}_2\text{CH}_3 > \text{CH}_3\text{OB}^+\text{OCH}_3 \gg \text{CH}_3\text{B}^+\text{CH}_3$. Furthermore, these findings are also in perfect agreement with the proposed reaction mechanism described in Scheme 1 because the oxygen lone pair participates in the nucleophilic ring reformation

step. This step not only is expected to be rate-limiting but also determines the final product ion structure.

The above reactions with $\text{CH}_3\text{OB}^+\text{OCH}_3$ reveal whether the substituent is located at the 2-position or at another ring position, thus distinguishing isomeric cyclic acetals and ketals. For example, 2-methyl-1,3-dioxolane is transformed to the cyclic boron cation of m/z 117 (Table 1) via loss of the 2-methyl group as part of the released neutral aldehyde. The 4-methyl substituent of 4-methyl-1,3-dioxolane remains, however, in the final tricoordinated boron cation, which therefore displays a m/z ratio 14 Th units higher than that of the corresponding ionic product from 2-methyl-1,3-dioxolane.

Although the isomers 4-methyl-1,3-dioxolane and 1,3-dioxane give isomeric C–O by B–O replacement boron

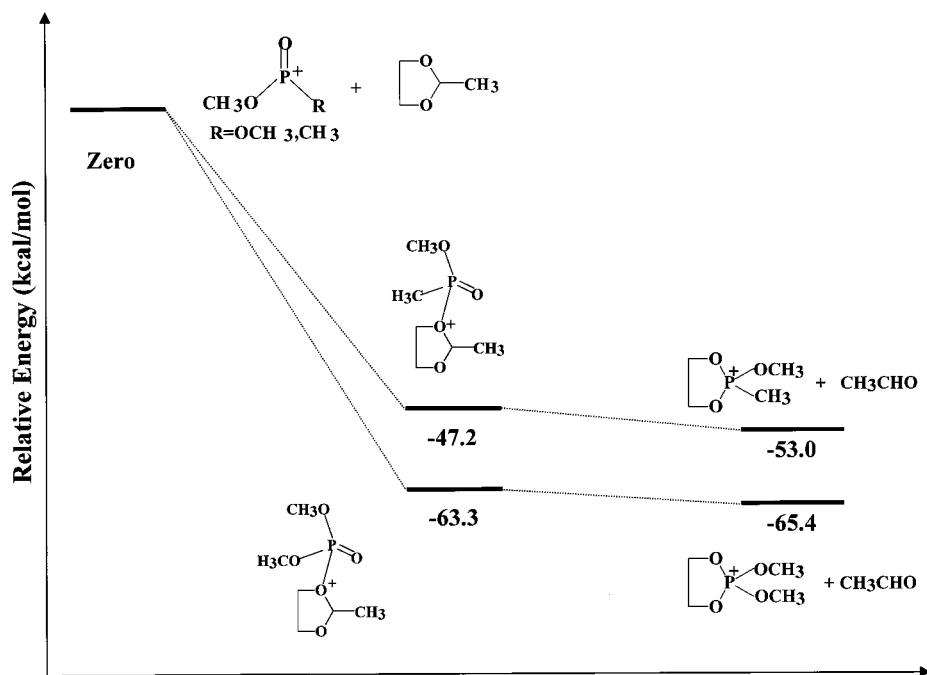


Figure 12. Intrinsic reaction coordinates (IRC) for the transacetalization reactions of $\text{CH}_3\text{P}^+(\text{O})\text{OCH}_3$ and $\text{CH}_3\text{OP}^+(\text{O})\text{OCH}_3$ with 2-methyl-1,3-dioxolane.

cations of m/z 131, they can nevertheless be distinguished. The six-membered cyclic boron cation from 1,3-dioxane displays a unique fragment ion of m/z 103 (Figure 3b), whereas the five-membered cyclic boron cation from 4-methyl-1,3-dioxolane reforms the reactant $\text{CH}_3\text{OB}^+\text{OCH}_3$ of m/z 73, exclusively. As proposed in Scheme 2, the five-membered cyclic boron cation dissociates to yield (i) $\text{CH}_3\text{OB}^+\text{OCH}_3$ by $\text{C}_2\text{H}_4\text{O}$ loss via the endocyclic C–O cleavage and (ii) $\text{C}_3\text{H}_7\text{O}^+$ by $\text{O}=\text{BOCH}_3$ loss via the endocyclic B–O cleavage. Meanwhile, the six-membered cyclic boron cation dissociates to yield $\text{CH}_3\text{OB}^+\text{OCH}_3$ by C_2H_4 loss followed by CH_2O loss via the endocyclic C–O cleavage predominantly (Scheme 3).

1.2. C–N or C–S by B–O Replacement. $\text{CH}_3\text{OB}^+\text{OCH}_3$ reacts moderately with thiazolidine (Figure 6a), a sulfur–nitrogen cyclic acetal, and so yields two ionic products of m/z 133 and m/z 116, likely via transacetalization-like mechanisms, with initial binding of the borinium ion at S and N, respectively. As nitrogen-containing compounds have been reported to have borinium ion affinities higher than those of sulfur-containing compounds,^{20,22,24,43} the approximately equal abundances of m/z 133 (S) and m/z 116 (N) is surprising. The intact adduct of m/z 162 was therefore submitted to collisional activation (Figure 6b) and was found to dissociate to several fragments: those of m/z 133, 130, 116, 102, and 73. The detailed fragmentation pathways are described in Scheme 4. The product ion distribution clearly establishes that the borinium ion preferentially binds to the N site of thiazolidine. The slightly larger abundance of the ion m/z 133 compared with that of the ion m/z 116 obtained from transacetalization reactions by initial S- and N-binding, respectively (Figure 6b), is probably due to the interfering dissociation channels of the N-binding borinium/thiazolidine adduct (Scheme 4). As expected, both product ions of m/z 133 and 116 fragment exclusively to reform the reactant ion $\text{CH}_3\text{OB}^+\text{OCH}_3$ (Figure 7).

1.3. Ab Initio Calculations. Tricoordinated boron cations are electronically and structurally intermediates

between the borinium cations and the neutral boranes. The interplay of σ - and π -bonding effects determines their structures and stabilities.⁴ To describe the thermodynamics of the above-demonstrated mechanism for transformation of acetals and ketals to the corresponding cyclic tricoordinated boron cations, the RHF/6-31G(d,p)-optimized structures of the cyclic tricoordinated boron cations were calculated and are presented in Figure 8. Typical endocyclic B–O, B–S, and B–N bond lengths in the optimized cyclic tricoordinated boron cations are 1.330, 1.795, and 1.384 Å, respectively. This result, which indicates the double-bond character of the endocyclic B–X (X = O, S, N) bond, is in excellent agreement with the available crystal structures of cyclic tricoordinated boron cations.⁴ The planar O–B–X (X = O, S, N) unit was also observed to maximize the $B_{p\pi}-X_{p\pi}$ bonding in the cyclic tricoordinated boron cations. The tricoordinated boron cation can be viewed to arise from the addition of a neutral base to a borinium ion, and consistent with this, the B–O bond in the original $\text{CH}_3\text{OB}^+\text{OCH}_3$ is stretched from 1.237 Å to an average value of 1.306 Å represented by the length of exocyclic B–O bond in the cyclic tricoordinated boron cation in Figure 8. Note that the CH_3O group, which is responsible for the recyclization, forms an even longer endocyclic B–OCH₃ bond (1.465 Å) in the product tricoordinated boron cation. These results can be explained by the fact that the tricoordinated boron cation has one less p orbital available for π -bonding, and thus, its π -bonding is much weaker than that of the borinium ion. Moreover, according to Mulliken charge analysis, the positive charge is mainly located on the boron atom and its magnitude falls in the range of +0.66 to +0.94. Meanwhile, typical charges on heteroatoms are 0.09, –0.39, and –0.56 for S, N, and O, respectively. This trend correlates with the electronegativity of the bonding heteroatom X (X = S, N, O).

Referring to the proposed mechanism shown in Scheme 1, calculated intrinsic reaction coordinates for reaction of $\text{CH}_3\text{OB}^+\text{OCH}_3$ with 2-methyl-1,3-dioxolane are shown

in Figure 9. The overall transacetalization-like reaction is estimated to be highly exothermic, by 43.3 kcal/mol. For reactions with thiazolidine (Figure 10), the overall transacetalization-like reaction initiated by binding at nitrogen is thermodynamically more favorable ($\Delta H_{\text{rxn}} = -25.5$ kcal/mol) than that initiated by binding at sulfur ($\Delta H_{\text{rxn}} = -17.7$ kcal/mol). Exactly as mentioned above, the larger relative abundance of the transacetalization product of m/z 133 generated by initial S-binding compared to that of m/z 116 generated by initial N-binding (Figure 6b) is the result of multiple competing dissociation channels described in Scheme 4. Note especially the thioxirane loss channel ($\Delta H_{\text{rxn}} = -37.0$ kcal/mol), a result of $\text{CH}_3\text{OB}^+\text{OCH}_3$ approaching the N site of thiazolidine.

The ab initio calculations (Figures 9 and 10) are consistent with the earlier suggestion that the second nucleophilic recyclization is the rate-limiting step. In comparison with oxygen acetals or ketals, the lower reaction efficiency of $\text{CH}_3\text{OB}^+\text{OCH}_3$ with thiazolidine is likely to be a result of the relatively larger dissociation barrier associated with the release of CH_2NH or CH_2S . With regard to the C–O by B–O replacement, the high efficiency displayed by the borinium ion is ultimately attributed to the initial formation of the strong B–O bond, which is estimated to be 39.5 ± 3.5 kcal/mol.¹³

2. Reactions with Phosphonium Ions. Analogously to acylium ions, phosphoryl-containing cations, such as $\text{CH}_3\text{P}^+(\text{O})\text{OCH}_3$ and $\text{CH}_3\text{OP}^+(\text{O})\text{OCH}_3$, transform cyclic acetals and ketals to the corresponding ionic P–O analogues of ketals.³¹ The ion/molecule reaction products are listed in Table 2. Interestingly, $\text{CH}_3\text{OP}^+(\text{O})\text{OCH}_3$, which is an isomer of $\text{CH}_3\text{P}^+(\text{O})\text{OCH}_3$, fails to react by transacetalization. As an addendum to our preliminary study,³¹ ab initio calculations were utilized to map the reaction pathway leading to the generation of 1,3,2-diheterophospholanium ions. Figure 11 displays the RHF/6-31G(d,p)-optimized geometries of various product 1,3,2-diheterophospholanium ions. Owing to the electronic and steric effects of the substituents, all the 1,3,2-diheterophospholanium ions exhibit distorted tetrahedral structures. The average angles of endocyclic O–P–O, O–P–S, and O–P–N are 98.9, 100.4, and 97.0°, respectively. This is understandable by the fact that five-membered rings in neutral pentaoxyphosphoranes invariably span apical-equatorial sites.^{33,44} The average bond lengths of endocyclic P–O, P–S, and P–N are estimated, however, to be 1.559, 2.044, and 1.617 Å, respectively. These lengths are consistent with typical X-ray crystallographic data for phosphonium salts.⁴⁵ Furthermore, it is interesting to note that those P^+-X bond lengths fall between the values for the corresponding single and double P^+-X bonds.⁴⁵ Hence, these endocyclic P^+-X bonds have some double-bond character with possible $p_\pi-d_\pi$ back-donation from the bonding heteroatom X to the phosphorus.

According to Mulliken charge analysis of the product 1,3,2-diheterophospholanium ion (Figure 11), the positive charge is heavily localized on the phosphorus atom (+1.36 to +1.79), and typical charges of the bonding heteroatoms are 0.02, –0.48, and –0.69 for S, N, and O, respectively. Note that the traditional description of the phosphoryl

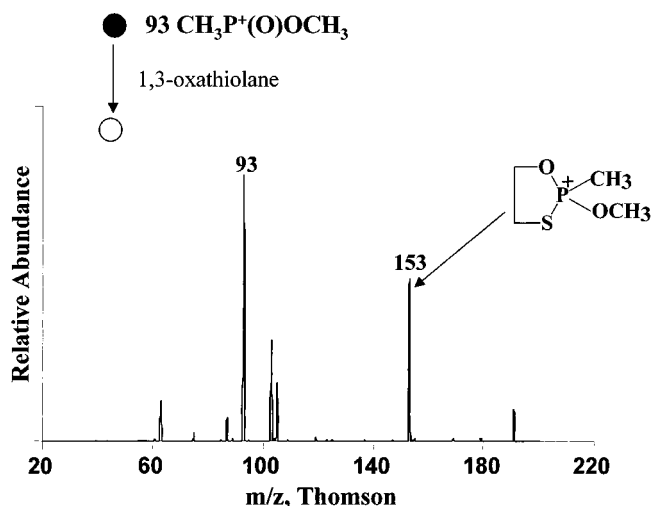


Figure 13. Product ion spectrum (MS^2) showing ion/molecule reactions of $\text{CH}_3\text{P}^+(\text{O})\text{OCH}_3$ with 1,3-oxathiolane.

group has been criticized frequently, and the phosphoryl group seems better represented as a resonance hybrid between singly and triply bonded structures. The thiophosphoryl bond can be viewed in the same manner but is rather weaker and contains less multiple-bond character than does the phosphoryl group.⁴⁶ The dominant dipolar σ bonding of P–S was also explored by natural bond orbital analysis (NBO) of protonated *O,O*-diethyl *O*-phenyl phosphorothionate.⁴⁷ Moreover, it has been reported that the “double bond” character for P^+-X in acyclic phosphonium ions decreases in the order $\text{X} = \text{N} > \text{O} > \text{S}$.⁴⁵ The Mulliken charge distribution here reported obviously supports the view that the P^+-X ($\text{X} = \text{N}, \text{O}, \text{S}$) bond is predominantly ionic.

Ab initio potential energy surfaces, taking the reactions of $\text{CH}_3\text{P}^+(\text{O})\text{OCH}_3$ and $\text{CH}_3\text{OP}^+(\text{O})\text{OCH}_3$ with 2-methyl-1,3-dioxolane as examples (see Figure 12), indicate that the initial electrophilic association is responsible for the overall high exothermicity of transformation of 2-methyl-1,3-dioxolane to its P–O analogue. Consistent with the experimental result, the transacetalization-like reaction of $\text{CH}_3\text{OP}^+(\text{O})\text{OCH}_3$ ($\Delta H_{\text{rxn}} = -65.4$ kcal/mol) is shown to be considerably more exothermic than that of $\text{CH}_3\text{P}^+(\text{O})\text{OCH}_3$ ($\Delta H_{\text{rxn}} = -53.0$ kcal/mol), which results probably from the higher stability of the tetraoxy-substituted phosphonium ion. Note also that the dissociation of the initial adducts to the product cyclic phosphonium ions are calculated to be 5.8 and 2.1 kcal/mol exothermic for $\text{CH}_3\text{P}^+(\text{O})\text{OCH}_3$ and $\text{CH}_3\text{OP}^+(\text{O})\text{OCH}_3$, respectively (Figure 12). Compared to that of the phosphonium ion, the relatively larger dissociation barrier of the borinium ion (Figure 9) is likely to result from the required stretching of the B–OCH₃ bond compared with that of the P–O bond in the recyclization step.

Reactions of both $\text{CH}_3\text{P}^+(\text{O})\text{OCH}_3$ and $\text{CH}_3\text{OP}^+(\text{O})\text{OCH}_3$ with thiazolidine display a regioselectivity that favors sulfur over nitrogen binding.³¹ To further verify this regioselectivity, the $\text{CH}_3\text{P}^+(\text{O})\text{OCH}_3$ ion was reacted with 1,3-oxathiolane. The reaction was expected to yield two transacetalization-like products resulting from initial

(44) Swamy, K. C. K.; Burton, S. D.; Holmes, J. M.; Day, R. O.; Holmes, R. R. *Phosphorus, Sulfur, Silicon* **1990**, *53*, 437.

(45) Imrie, C.; Modro, T. A.; Van Rooyen, P. H.; Wagener, C. C. P.; Wallace, K. *J. Phys. Org. Chem.* **1995**, *8*, 41.

(46) Schmidt, M. W.; Gordon, M. S. *J. Am. Chem. Soc.* **1985**, *107*, 1922.

(47) Kuivalainen, T.; Kostianen, R.; Uggla, R.; Sundberg, M. R.; Björk, H. *J. Am. Soc. Mass Spectrom.* **1996**, *7*, 189.

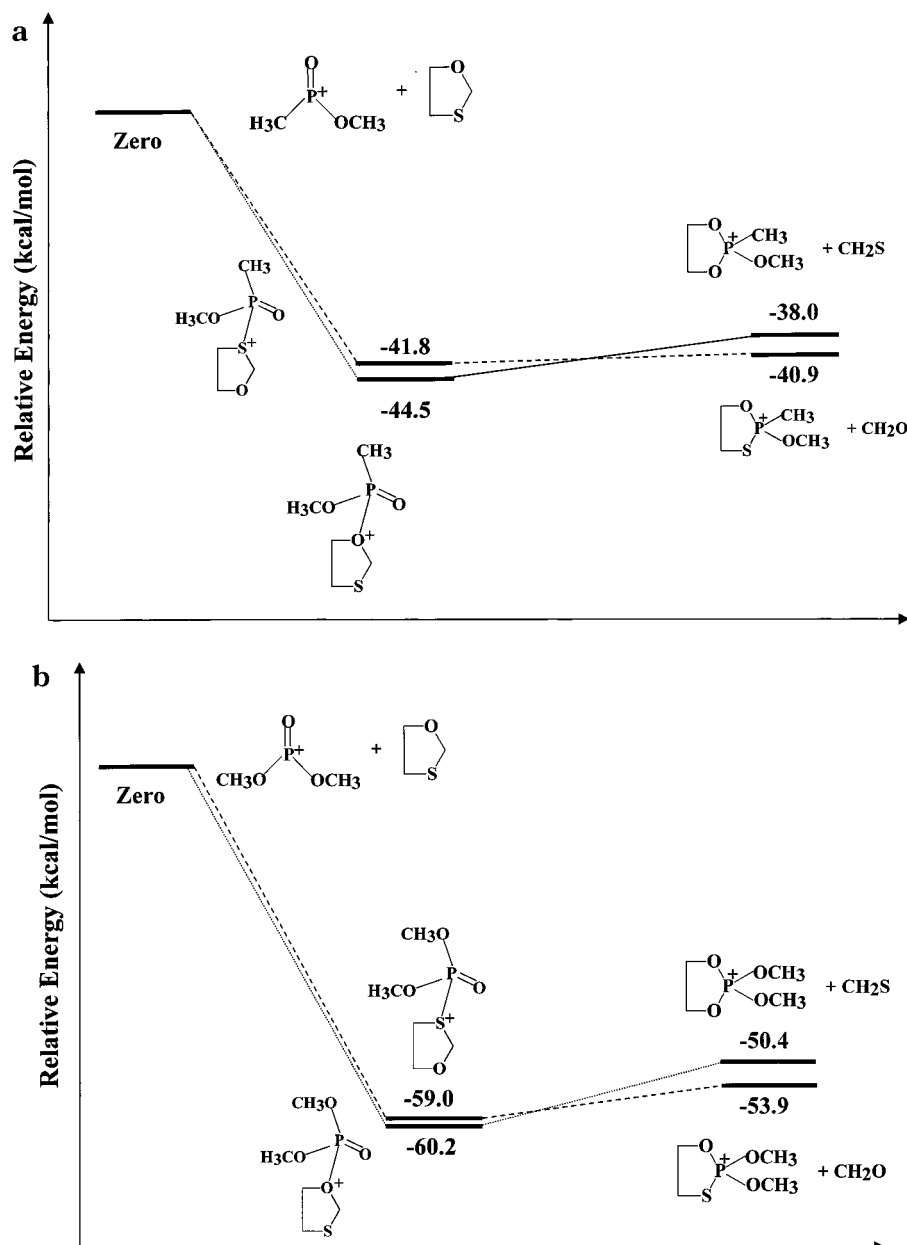


Figure 14. Intrinsic reaction coordinates (IRC) for the transacetalization reactions of (a) $\text{CH}_3\text{P}^+(\text{O})\text{OCH}_3$ and (b) $\text{CH}_3\text{OP}^+(\text{O})\text{OCH}_3$ with 1,3-oxathiolane showing the regioselectivity at S site over O site.

phosphorylation at O or S. But surprisingly, only the transacetalization-like product, m/z 153, resulting from initial phosphorylation at S was formed (Figure 13). This result suggests that the S site of 1,3-oxathiolane is almost exclusively attacked. On the basis of the calculations (Figure 14a), the observed regioselectivity is clearly explained by the much smaller activation barrier of the recyclization step when initial phosphorylation is at S ($E_{\text{act}} = 0.9$ kcal/mol) than at O ($E_{\text{act}} = 6.5$ kcal/mol). It is this activation barrier that makes the transacetalization reaction initiated by phosphorylation at S ($\Delta H_{\text{rxn}} = -40.9$ kcal/mol) more exothermic than that initiated by phosphorylation at O ($\Delta H_{\text{rxn}} = -38.0$ kcal/mol). This is also the case for reaction of $\text{CH}_3\text{OP}^+(\text{O})\text{OCH}_3$ with 1,3-oxathiolane (Figure 14b). Therefore, the regioselectivity of phosphoryl-containing cations falls in the order of $\text{S} > \text{N} > \text{O}$. As the phosphoryl-containing cations are hard ionic Lewis acids, the regioselectivity displayed cannot be explained by the hard-soft acid-base (HSAB) prin-

ciple.^{48,49} It is suggested that this regioselectivity is strongly dependent on the leaving ability of the released neutral molecule, which has been suggested to be in the order of $\text{CH}_2\text{O} > \text{CH}_2=\text{NH} > \text{CH}_2\text{S}$ in the gas phase,⁵⁰ that is to say, on the stability of the 1,3,2-diheterophospholanium ion. When subjected to CID (Figure 15a), the product 2-methoxy-2-methyl-1,3,2-oxathiophospholanium ion of m/z 153 dissociates to regenerate the initial reactant ion $\text{CH}_3\text{P}^+(\text{O})\text{OCH}_3$, m/z 93, and its thioanalogue $\text{CH}_3\text{P}^+(\text{S})\text{OCH}_3$, m/z 109 under the assumption of the absence of a thiono-thiolo rearrangement via methyl migration. Similar dissociation behavior (Figure 15b) is shown by the product 2,2-dimethoxy-1,3,2-oxathiophospholanium ion of m/z 169 obtained by reaction of $\text{CH}_3\text{OP}^+(\text{O})\text{OCH}_3$ with 1,3-oxathiolane. Note that the

(48) Pearson, R. G. *J. Am. Chem. Soc.* **1963**, *85*, 3533.

(49) Pearson, R. G. *J. Am. Chem. Soc.* **1988**, *110*, 7684.

(50) Pau, J. K.; Kim, J. K.; Caserio, M. C. *J. Am. Chem. Soc.* **1978**, *100*, 3838.

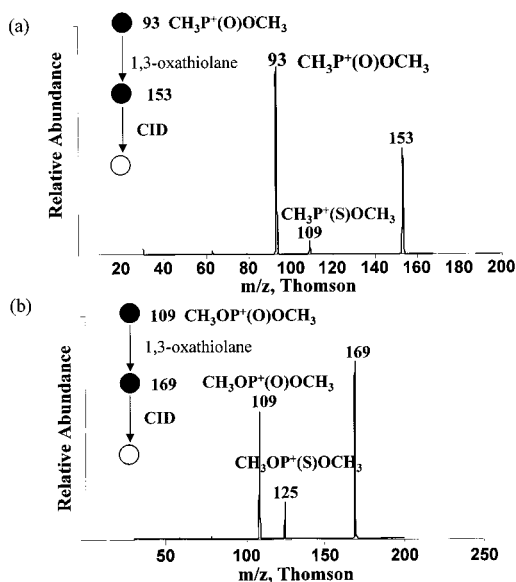


Figure 15. Sequential product ion (MS^3) spectrum of the product 1,3,2-oxathiophospholanium ion of reaction of 1,3-oxathiolane with (a) $\text{CH}_3\text{P}^+(\text{O})\text{OCH}_3$ and (b) $\text{CH}_3\text{OP}^+(\text{O})\text{OCH}_3$.

reaction provides a reversible route for $\text{RRP}^+=\text{O}$ to $\text{RRP}^+=\text{S}$ conversion. In contrast, the corresponding cyclic “ionic thioketals” formed on reactions of thioacylium ions with acetals and ketals dissociate exclusively back to the acylium ion due to the greater electronic stability of the acylium ion.^{41,51} The dissociation behavior of the product 1,3,2-oxathiophospholanium ions observed in this study (Figure 15) also suggests that the stability difference between the phosphoryl- vs thiophosphoryl-containing cations is smaller than that of carbonyl- vs thiocarbonyl-containing cations.

Conclusions

The dimethoxyborinium ion reacts with a variety of cyclic acetals and ketals, and with thiazolidine, to generate stable cyclic tricoordinated boron cations in high yield via a mechanism similar to the Eberlin transacetalization of acylium ions. This reaction can be used to distinguish isomeric acetals and ketals with regard to the positions of substituents and ring size. The tricoordinated boron cations with five-membered rings dissociate by $\text{C}_2\text{H}_4\text{O}$ loss and by $\text{O}=\text{BOCH}_3$ loss via endocyclic C–O and B–O cleavage, respectively; those with six-membered rings dissociate only by C_2H_4 loss via endocyclic C–O cleavage. Intramolecular nucleophilic-induced cyclization is the rate-limiting step in the proposed reaction mechanism (Scheme 1), and the reactivities of the borinium ions fall in the order of $\text{CH}_3\text{OB}^+\text{C}_2\text{H}_5 > \text{CH}_3\text{OB}^+\text{OCH}_3 > \text{CH}_3\text{B}^+\text{CH}_3$. Compared with the acylium and phosphonium ions, the dimethoxyborinium ion shows weaker regioselectivity in reactions with acetal analogues with two different basic sites, probably due to its greater Lewis acidity. The transacetalization-like reaction exothermicity is governed by the strength of the initial B–O bonding.

(51) Caserio, M. C.; Kim, J. K. *J. Am. Chem. Soc.* **1983**, *105*, 6896.

Although the phosphoryl group is more polar and suffers greater solvation effects than the carbonyl group in the condensed phase, phosphoryl-containing cations, such as $\text{CH}_3\text{OP}^+(\text{O})\text{CH}_3$ and $\text{CH}_3\text{OP}^+(\text{O})\text{OCH}_3$, can also undergo structurally diagnostic transacetalization-like reactions with acetals and ketals to generate 1,3,2-diheterophospholanium ions. From the data for 1,3-oxathiolane and thiazolidine, transacetalization-like reactions by the phosphonium ions show strong regioselectivity in the order of $\text{S} > \text{N} > \text{O}$. This reactivity of the phosphoryl group is expected to be useful to monitor organophosphorus esters at trace levels and probably offers an alternative way to study phosphoryl transfer process by mass spectrometry.

Cyclic acetals and ketals are the most common protective groups for diols and carbonyl compounds in organic synthesis.⁵² The deprotection of acetals and ketals is usually accomplished by aqueous acid hydrolysis. For substrates possessing acid-sensitive functionalities, methods using nonacidic and anhydrous conditions have received much attention. These include use of transition metals and Lewis acids,^{53,54} oxidative methods,⁵⁵ phosphorus-based reagents,^{56,57} and silicon-based reagents.⁵⁸ Parallel to this ongoing search for nonaqueous deprotecting reagents and the study of their corresponding regioselectivity in the condensed phase, this study explicitly explores the deprotecting mechanism involving a Lewis acid–base complex and establishes the “soft” nature of these deprotecting reagents, which is mainly due to the greater polarity of the B–O or P–O bond, in comparison with that of C–O bond.

To conclude, cations with dual acidity and basicity are capable of undergoing transacetalization-like reactions with acetals and ketals. The reaction enthalpy is predominantly governed by the initial association, i.e., by the Lewis acidity of the reactant cation. The regioselectivity of the transacetalization reaction is, however, heavily dependent on the stability of the product “ionic ketal”. This transacetalization methodology is currently being extended to transition-metal systems.

Acknowledgment. The work at Purdue was supported by the National Science Foundation, Grant No. CHE 97-32670, and the U.S. Department of Energy, Basic Energy Sciences. The Research at UNICAMP was supported by the Research Support Foundation of the State of São Paulo (FAPESP) and the Brazilian National Research Council (CNPq).

JO982446S

(52) Greene, T. W.; Wuts, P. G. M. *Protecting Groups in Organic Synthesis*, 2nd ed.; John Wiley & Sons: New York, 1991.

(53) Gros, P.; LePerchec, P.; Senet, J. P. *J. Chem. Res., Synop.* **1995**, 196.

(54) Ma, S.; Venanzi, L. M. *Tetrahedron Lett.* **1993**, *34*, 8071.

(55) Nishiguchi, T.; Ohosima, T.; Nishida, A.; Fujisaki, S. *J. Chem. Soc., Chem. Commun.* **1995**, 1121.

(56) Denis, J.-N.; Krief, A. *Angew. Chem., Int. Ed. Engl.* **1980**, *19*, 1006.

(57) Johnstone, C.; Kerr, W. J.; Scott, J. S. *Chem. Commun.* **1996**, 341.

(58) Kaur, G.; Trehan, A.; Trehan, S. *J. Org. Chem.* **1998**, *63*, 2365.